A Performance Evaluation of the World Wide Lightning Location Network (WWLLN) over the Tibetan Plateau

PENGLEI FAN,[a,b] DONG ZHENG,[a,b] YIJUN ZHANG,[a,b,c] SHANQIANG GU,[d] WENJUAN ZHANG,[a,b] WEN YAO,[a,b] BIWU YAN,[d] AND YONGBIN XU[e]

[a] *State Key Laboratory of Severe Weather, Chinese Academy of Meteorological Sciences, Beijing, China*
[b] *Laboratory of Lightning Physics and Protection Engineering, Chinese Academy of Meteorological Sciences, Beijing, China*
[c] *Institute of Atmospheric Sciences, Fudan University, Shanghai, China*
[d] *Wuhan NARI Co., Ltd., State Grid Electric Power Research Institute, Wuhan, China*
[e] *Lightning Protection Center of Tibet Autonomous Region, Lhasa, China*

(Manuscript received 25 August 2017, in final form 19 February 2018)

ABSTRACT

A systematic evaluation of the performance of the World Wide Lightning Location Network (WWLLN) over the Tibetan Plateau is conducted using data from the Cloud-to-Ground Lightning Location System (CGLLS) developed by the State Grid Corporation of China for 2013–15 and lightning data from the satellite-based Tropical Rainfall Measuring Mission (TRMM) Lightning Imaging Sensor (LIS) for 2014–15. The average spatial location separation magnitudes in the midsouthern Tibetan Plateau (MSTP) region between matched WWLLN and CGLLS strokes and over the whole Tibetan Plateau between matched WWLLN and LIS flashes were 9.97 and 10.93 km, respectively. The detection efficiency (DE) of the WWLLN rose markedly with increasing stroke peak current, and the mean stroke peak currents of positive and negative cloud-to-ground (CG) lightning detected by the WWLLN in the MSTP region were 62.43 and −56.74 kA, respectively. The duration, area, and radiance of the LIS flashes that were also detected by the WWLLN were 1.27, 2.65, and 4.38 times those not detected by the WWLLN. The DE of the WWLLN in the MSTP region was 9.37% for CG lightning and 2.58% for total lightning. Over the Tibetan Plateau, the DE of the WWLLN for total lightning was 2.03%. In the MSTP region, the CG flash data made up 71.98% of all WWLLN flash data. Based on the abovementioned results, the ratio of intracloud (IC) lightning to CG lightning in the MSTP region was estimated to be 4.05.

1. Introduction

The Tibetan Plateau has always been a key topic in atmospheric science research because, as the area with the highest average elevation in the world, its thermal and dynamical effects have a significant influence on global circulation and climate (Flohn and Reiter 1968; Yanai and Li. 1994). Convective activity over the plateau is important for the transport of material between the troposphere and stratosphere, the radiation budget, and precipitation downstream of the plateau. However, there are few meteorological stations on the plateau and they are unevenly distributed because the plateau is sparsely populated and exposed to extreme environments. In addition, the mountainous terrain over the plateau limits the coverage of weather radars, and at present satellite observations have relatively low spatiotemporal resolution. These factors limit observation of the short-lived and small-scale convective processes that dominate over the plateau. As one of the most important weather phenomena that accompany strong convection, lightning is often used to diagnose changes in convection, and observations of lightning may play a unique role in monitoring the wide-ranging convective activities over the Tibetan Plateau.

At present, lightning detection data over the Tibetan Plateau are mainly provided by spaceborne lightning optical sensors, as well as the ground-based Cloud-to-Ground Lightning Location System (CGLLS) and the World Wide Lightning Location Network (WWLLN).

Both the China Meteorological Administration and China State Grid Corporation have installed lightning location systems that cover most parts of China

Corresponding authors: Dong Zheng, zhengdong@cma.gov.cn; Yijun Zhang, zhangyijun@fudan.edu.cn

DOI: 10.1175/JTECH-D-17-0144.1

(e.g., Chen et al. 2002, 2012; Yang et al. 2015; Xia et al. 2015). On the Tibetan Plateau, however, these systems are mainly located in the mideastern part of the plateau because of constraints such as population distribution and electric power supply. Therefore, these systems have limited ability to detect the lightning that occurs over the middle and western areas of the plateau.

Spaceborne lightning optical detection systems, such as the Optical Transient Detector (OTD, from 1995 to 2000) on the *OrbView-1* satellite (formerly *Microlab-1*) or the Lightning Imaging Sensor (LIS, from 1997 to 2015) on the Tropical Rainfall Measuring Mission (TRMM), can detect total [intracloud (IC) and cloud-to-ground (CG)] lightning and have a large spatial coverage. For example, the LIS can monitor lightning flashes south of 38°N in the plateau region, and the OTD can observe the whole plateau. However, the LIS and the OTD are both on polar-orbiting satellites, meaning that a given location is observed only for a short time in each orbit; for example, the observation time of flashes in a fixed location by the LIS in a given orbit is only about 90 s. In addition, a new geostationary satellite named *Fengyun-4* equipped with a lightning imager and having the capability of observing lightning nearly throughout all China was recently launched in 2016 and is expected to play an important role in imaging the lightning in the plateau in the future (Cao. 2016).

The WWLLN is operated by the University of Washington and can continuously detect global lightning activity. To some extent, the WWLLN overcomes both the lack of spatial coverage of the regional ground-based lightning detection network and the lack of temporal coverage of the spaceborne lightning optical detection system. The long time series of WWLLN lightning data has great value in understanding plateau lightning characteristics, especially in comparing lightning and convective activities between different parts of the plateau, or even between the plateau and other regions. Furthermore, WWLLN lightning data also can be used to test the performance of the lightning imager loaded by *Fengyun-4* (Cao. 2016) over the Tibetan Plateau.

Overall though, the detection efficiency (DE) and location accuracy (LA) of the WWLLN are relatively low, and these two parameters must be considered when using the data. Previous studies have reported that the performance of the WWLLN varies significantly with location (e.g., Abarca et al. 2010; Abreu et al. 2010; Thompson et al. 2014). It is therefore necessary to carry out specific studies in different regions. This study compares WWLLN data with CG lightning data from the CGLLS and with total lightning data from the LIS to evaluate the performance of the WWLLN over the Tibetan Plateau.

2. Data sources

a. WWLLN

The WWLLN developed by the University of Washington has sensors installed on a global scale and can locate lightning events worldwide. The sensors operate in the very low frequency (VLF) band of 3–30 kHz and detect electromagnetic radiation pulses emitted by lightning strokes up to several thousands of kilometers away. At present, at least five sensors are needed to detect a stroke to determine the location using time of group arrival (TOGA) technology (Dowden et al. 2002, 2008; Hutchins et al. 2012). The number of WWLLN sensors has increased gradually since its establishment (Lay et al. 2004; Hutchins et al. 2013) and has reached more than 70 by 2017 (http://wwlln.net/). Previous studies have compared regional WWLLN detection with other ground-based networks and assessed the performance of the WWLLN (e.g., Lay et al. 2004; Rodger et al. 2004, 2005, 2006; Jacobson et al. 2006; Abarca et al. 2010; Abreu et al. 2010). These studies noted that the WWLLN detected both CG lightning strokes and large IC pulses, and it was most sensitive to high-peak-current lightning strokes. Overall, the performance of the WWLLN has improved over time as a result of the increasing number of sensors (Abarca et al. 2010) and improvements in waveform processing algorithms (Rodger et al. 2009). Early studies often found WWLLN's DE for total lightning to be less than 1% and the DE for CG lightning to be less than 2%, with LA no better than 20 km (Lay et al. 2004; Rodger et al. 2004; Jacobson et al. 2006). In Canada, by 2008–09 WWLLN's DE for total lightning was 6.19%, for CG lightning 10.3%, and the LA was better than 10 km (Abreu et al. 2010). By comparing WWLLN "strokes" with LIS "flashes," Rudlosky and Shea (2013) indicated that WWLLN's DE in the Western Hemisphere for total lightning increased from 3% in 2009 to 9.2% in 2012. They reported that the average spatial and time differences were 11 km and 62 ms, respectively. Bürgesser (2017) found that the global average WWLLN's DE relative to the LIS was about 7.2% during 2012–14. Thompson et al. (2014) compared WWLLN "strokes" with LIS "groups" and found obvious differences in WWLLN's DE in different regions of the Western Hemisphere. Generally, the WWLLN could detect 11% of LIS groups.

Three years (2013–15) of the WWLLN dataset are used in this research. Referring to Fig. 1 in Soula et al. (2016),

during this period only two new sensors far away from the plateau were added to WWLLN in Asia in 2013. Therefore, the performance of the WWLLN over the plateau is assumed to be consistent through 2013–15. The dataset includes CG lightning strokes and IC pulses and cannot differentiate between them. The occurrence time, longitude, latitude, and other parameters are given in the datasets; the time precision is 1 μs. The WWLLN strokes are grouped into flashes using the criteria that adjacent strokes for one flash should be within an interval of 0.5 s and a distance of 30 km, which will be primarily used to get the components (IC flashes and CG flashes) of the WWLLN data and serve for the estimation of Z value (IC flashes/CG flashes) over the plateau (section 5).

b. CGLLS

The CGLLS built and operated by the State Grid Corporation of China is chosen for the comparison in this study. There were 108 stations in Qinghai and Tibet by 2017 (Fig. 1). Its dataset contains information on located lightning strokes, such as precise time, latitude, longitude, polarity, and peak current. The CGLLS uses both magnetic detection and time-of-arrival (TOA) location methods to locate the lightning strokes (Chen et al. 2002). By investigating the waveform shape of strokes, the CGLLS was designed to locate only the return strokes of CG lightning flashes, although it was nearly inevitable but should be rare that some IC lightning stokes may be misidentified as CG lightning strokes. Following previous studies (e.g., Cummins et al. 1998), positive CG lightning strokes with current less than 10 kA were removed from the CGLLS dataset because of a possible misinterpretation of cloud lightning. It is then assumed that the rest of the CGLLS stroke data were all contributed by return strokes of CG lightning flashes. Three years (2013–15) of the CGLLS stroke data over the plateau were used in this research. We chose the reprocessing data (also provided by the State Grid Corporation of China), which seemed to be of better quality than the real-time data, by increasing the recordings that were previously out of consideration because of the delay in real-time data transmission and by removing some clearly wrong positioning in real-time data. The original return stroke data of the CGLLS were grouped based on the criterion that adjacent return strokes for one lightning flash should occur within an interval of 0.5 s and a distance of 10 km (Zheng et al. 2016). The location of the first return stroke was taken as the position of the CG flash.

No study on the performance of the CGLLS over the plateau is found. But the performance of the CGLLS in Guangdong Province, China, which is also operated by the State Grid Corporation of China and has exactly the same detection principle, parameter settings, location algorithms, and hardware as the CGLLS over the plateau, has been checked and can be used for reference. Chen et al. (2012) evaluated the CGLLS in Guangdong with observations of triggered lightning flashes and natural lightning flashes on tall structures. The results showed that the CG flash detection efficiency and CG stroke detection efficiency were about 94% and 60%, respectively. The arithmetic mean and median values for location error were estimated to be about 710 and 489 m, respectively. The absolute percentage errors of peak current estimation were within 0.4%–42%, with arithmetic mean and median values of about 16.3% and 19.1%, respectively.

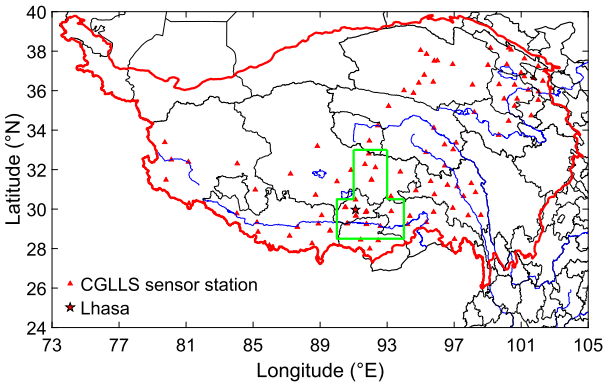

FIG. 1. Spatial distribution of CGLLS stations in Qinghai and Xizang Provinces in 2017. CGLLS stations (red triangles) and the location of Lhasa (star), the capital of Xizang Province, are marked. The boundary of the Tibetan Plateau in China is denoted (red line; Zhang et al. 2002). The region of high detection efficiency determined in section 3a is denoted (green line).

c. LIS

The LIS is an instrument on the TRMM satellite that was launched in November 1997 with an orbital inclination of 35° and an initial altitude of 350 km. Its orbit was subsequently boosted to 403 km in 2001 to increase mission lifetime, and the LIS ceased observation in 2015. The LIS used a charge-coupled device (CCD) array of 128 × 128 pixels, which, combined with the use of a wide-angle lens, gave a field of view of 600 km × 600 km on Earth's surface with a spatial resolution of between 3 and 6 km (Christian et al. 1999; Cecil et al. 2014). The orbit and field of view limited LIS observations to a band between 38°N and 38°S.

Using a clustering algorithm, the lightning detected by the LIS is classified into four parts: events, groups, flashes, and areas. An event is defined as a single pixel exceeding the background threshold during a single 2-ms time frame. A group comprises adjacent multiple events that occur in the same 2-ms time frame. A flash,

the most important parameter, is defined as a cluster of groups within 5.5 km and 330 ms of each other. An area consists of a set of flashes separated in space by no more than 16.5 km, which is similar to the size of a thunderstorm cell (Christian et al. 2003; Mach et al. 2007).

By comparing LIS and Lightning Detection and Ranging (LDAR) data, Ushio et al. (2002) found that the mean location differences between IC and CG flashes were 4.3 and 12.2 km, respectively. Boccippio et al. (2002) found a DE of 88 ± 9% for the LIS, made up of a daytime value of 73 ± 11% and a nighttime value of 93 ± 4%.

The present study uses the LIS orbit "flash" data for 2013–14. The dataset contains not only the occurrence time and location, but also the radiant energy of total lightning events, duration time, pixel area, and the number of inclusive groups or events.

3. Data processing and methods

a. Matching between WWLLN and CGLLS

The WWLLN performance for CG lightning was evaluated by comparing WWLLN data with CGLLS data. As CGLLS sensors were more densely distributed in the middle Tibetan Plateau during the analysis period, we first selected that region, which is also considered to cover the lightning hot spot over the plateau (Qie and Toumi 2003; Qi et al. 2016), to ensure high-quality CGLLS data. To further ensure the high DE of the CGLLS, we analyzed the spatial distribution of minimum detectable peak current determined by the CGLLS during 2013–15 (Fig. 2). Note that the lower the minimum detectable peak current, the higher the DE is for the CGLLS in the region. We finally chose the area surrounded by the red line in Fig. 2 as the comparison region, where the minimum detectable peak current was generally less than 4 kA. Below, we refer in particular to this region as the middle-southern Tibetan Plateau (MSTP) region. Zheng et al. (2016) exhibited the spatial distribution of the minimum detected peak current of the CGLLS in Guangdong Province (see their Fig. 3). The magnitude of the minimum detected peak current over Guangdong Province is generally the same as that over the MSTP region. Considering again the same technology, the algorithm and hardware of the CGLLS in the plateau and that in the Guangdong Province (also see in section 2b), we will think of the performance of the CGLLS over Guangdong given by Chen et al. (2012) (also see in section 2b) as that of the CGLLS over the MSTP region.

In previous research, coincident lightning between the WWLLN and other sources of data is identified by establishing a matching time/space window, within which

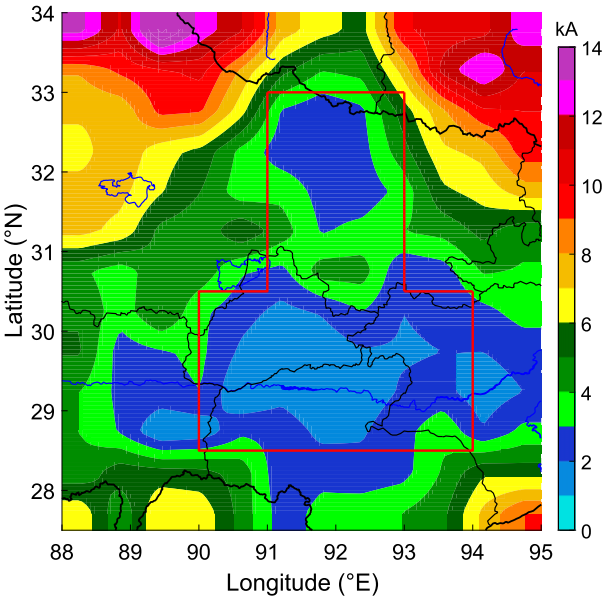

FIG. 2. Spatial distribution of the minimum detectable peak current determined by the CGLLS in the middle Tibetan Plateau area. The region of comparison between the CGLLS and the WWLLN (red line; shown in green in Fig. 1) is denoted. A lower minimum detectable peak current corresponds to a higher DE of the CGLLS in this region.

an event reported by both networks is defined to be coincident (e.g., Lay et al. 2004; Rodger et al. 2004, 2005, 2006; Jacobson et al. 2006; Abarca et al. 2010; Abreu et al. 2010). Two kinds of matches were made here. 1) WWLLN strokes (including IC pulses and CG return strokes) that matched CGLLS CG return strokes. Theoretically, WWLLN detects strong discharges, so it is reasonable to assume that the CG lightning strokes detected by the WWLLN would also be detected by the CGLLS. If a WWLLN stroke and a CGLLS return stroke lay within time and space windows of 0.5 ms and 50 km, respectively, they were regarded as coincident. If more than one CGLLS return stroke matched the same WWLLN stroke (this rarely happened in practice, 0.75% of all), then the closest CGLLS record in time would be chosen as the matched record. 2) WWLLN strokes that matched CGLLS flashes. In this case the time and space windows were 1 s and 50 km, respectively, and it was possible for several WWLLN strokes to match the same CGLLS flash. If so, these WWLLN strokes would be considered as belonging to a CG lightning flash. While if a WWLLN stroke could not match any CGLLS flash, then the stroke record is considered as an IC pulse. Given the rough environment and severe conditions over the Tibetan Plateau, if the WWLLN detected a stroke event but the CGLLS did not detect any lightning location record 0.5 h before or after the event, then the WWLLN stroke

TABLE 1. Matching results between the WWLLN and the CGLLS in the MSTP region. The stroke (flash) coincidence percentage is calculated by dividing the number of stroke (flash) coincidences by the number of all CGLLS strokes (flashes).

	2013	2014	2015	Total
WWLLN strokes	27 118	27 489	26 498	81 105
CGLLS return strokes	205 085	255 065	185 408	645 558
WWLLN–CGLLS stroke coincidences	16 829	17 578	12 727	47 134
Stroke coincidence percentage	8.21	6.89	6.86	7.30
CGLLS CG lightning flashes	150 844	186 367	111 933	449 144
WWLLN–CGLLS flash coincidences	15 701	16 386	12 675	44 762
Flash coincidence percentage	10.41	8.79	11.32	9.97

was removed to prevent adverse effects caused by a fault or anomalous operating conditions of the CGLLS. If a WWLLN flash includes any stroke belonging to a CG lightning flash (determined during the second kind of match), it was regarded as a WWLLN CG lightning flash; otherwise, it was regarded as a WWLLN IC lightning flash.

b. *Matching between WWLLN and LIS*

LIS flash data were compared with WWLLN stroke data for the whole Tibetan Plateau region, with the matching method similar to that used for the CGLLS. Using LIS flash data as a background sample, a flash that matched with a WWLLN stroke was considered as the same event reported by both networks. The time and space matching criteria were selected as 330 ms and 25 km, respectively, following Rudlosky and Shea (2013). These matching criteria were developed to avoid double counting as much as possible. If a LIS flash matched multiple WWLLN strokes, then the closest WWLLN record in time was used to obtain the occurrence time and location of the WWLLN stroke.

4. Comparisons of different observation data

a. *Comparison of WWLLN and CGLLS*

During 2013–15 in the MSTP region (Fig. 2), the CGLLS detected 449 144 flashes, including 645 558 return strokes, and WWLLN detected 62 185 flashes (not shown), including 81 105 strokes (Table 1). The number of flashes and strokes recorded by the CGLLS that were matched by the WWLLN were 44 762 and 47 134, respectively. Using the coincidence data for the 47 134 strokes, Fig. 3 shows the time difference (Fig. 3a) and spatial-separation magnitude (Fig. 3b) between matched strokes (WWLLN minus CGLLS). The time difference is roughly symmetric about zero, and the mean time difference is $-8.4\,\mu$s with a standard deviation of $46.6\,\mu$s. In contrast, Abreu et al. (2010) found that the mean value of time difference between WWLLN and Canadian Lightning Detection Network (CLDN) was $-6.4\,\mu$s; 95.8% of the absolute values of the time difference are within 0.1 ms and 99.5% are within 0.2 ms. The mean latitudinal spatial-separation

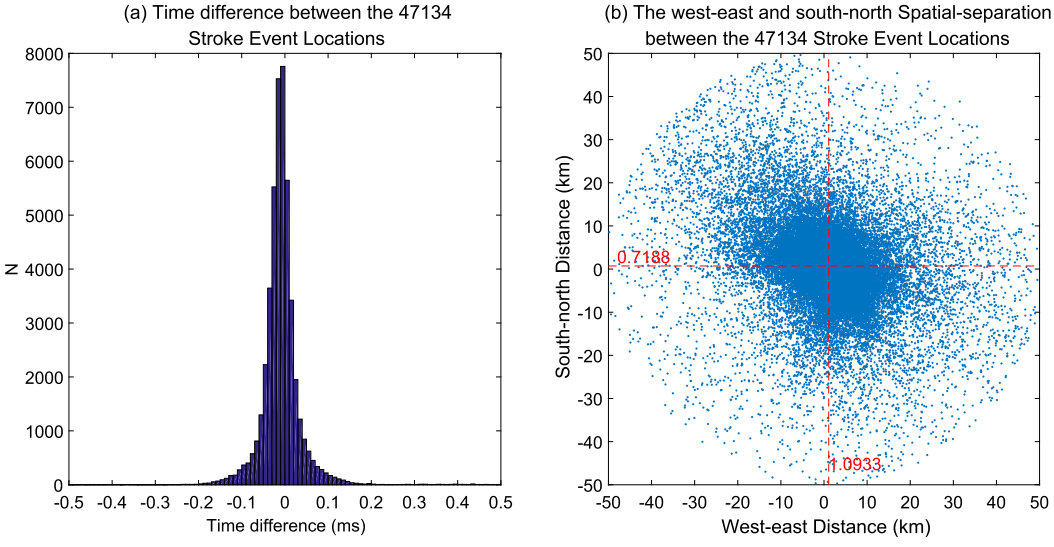

FIG. 3. (a) Time difference and (b) spatial-separation magnitudes between the 47 134 matched WWLLN and CGLLS strokes (WWLLN minus CGLLS) during 2013–15. The mean time difference and spatial-separation magnitudes are $-8.4\,\mu$s and 9.97 km, respectively. Data are grouped into 0.01-ms bins in (a), and (b) shows the mean south–north and west–east spatial-separation magnitudes (two dashed red lines).

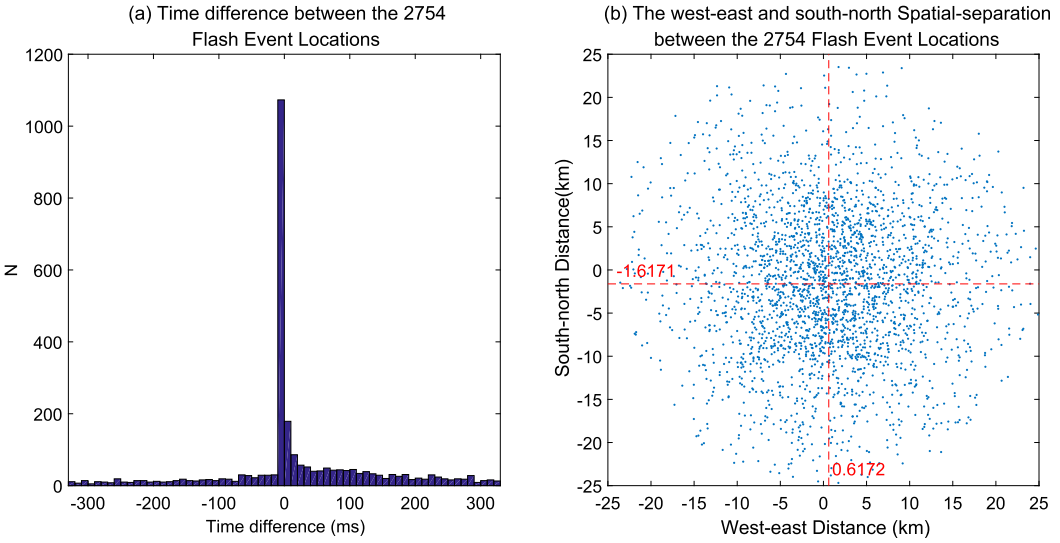

FIG. 4. (a) Time difference and (b) spatial-separation magnitudes between the 2754 matched WWLLN strokes and matched LIS flashes (WWLLN minus LIS) during 2013–14. The mean time difference and spatial-separation magnitudes are 21.84 ms and 10.93 km, respectively. Data are grouped into 0.01-bin-sizes in (a), and (b) shows the mean south–north and west–east spatial-separation magnitudes (two dashed red lines).

magnitude is 1.09 km with a standard deviation of 9.96 km, and the mean longitudinal spatial-separation magnitude is 0.72 km with a standard deviation of 9.44 km, as shown in Fig. 3b. In addition, 87.1% of the spatial-separation magnitudes are less than 20 km and 94.2% are less than 30 km. Note that the CGLLS has relatively high LA (mean and median location errors are 710 m and 489 m, respectively; Chen et al. 2012), so we can use the CGLLS locations as the reference value. In this case the mean LA of the WWLLN in the MSTP region is 9.97 km with a standard deviation of 9.54 km, and the geometric and median location errors are 6.67 and 6.61 km, respectively. The distribution of the time difference and spatial-separation magnitude indicates that the matching method is credible.

Table 1 also shows that the percentage of CGLLS strokes matched by the WWLLN in all CGLLS stroke data ranges from 6.86% to 8.21%, with a 3-yr mean value of 7.30%. The corresponding values for CG lightning flashes are 8.79%–11.32%, with a mean value of 9.97%.

b. *Comparison of WWLLN and LIS*

During 2013–14, the LIS observed 113 970 flashes in the rectangular region shown in Fig. 1 (the Tibetan Plateau and surrounding area), 2754 of which were matched by the WWLLN. Similar to Fig. 3, Fig. 4 shows the distribution of time difference (Fig. 4a) and spatial-separation magnitudes (Fig. 4b) between LIS flashes and the matched WWLLN strokes (WWLLN minus LIS). Figure 4a indicates that the peak time difference is concentrated in the −10- to 0-ms interval, but there are more positive values than negative values. It may be attributed to the fact that the LIS flash occurrence time is that of the first observed event, while the flash stroke observed by WWLLN can occur during the discharge process. The mean time difference is 21.84 ms with a standard deviation of 116.27 ms. The mean longitudinal and latitudinal spatial-separation magnitudes are −1.62 and 0.62 km, respectively, with standard deviations of 8.69 and 8.56 km, respectively. The absolute spatial-separation magnitude is 10.93 km with a standard deviation of 5.92 km. In contrast, Rudlosky and Shea (2013) found the average time difference and spatial-separation magnitudes between the WWLLN and the LIS were 62 ms and 11 km, respectively, which also indicates that the matching method we used is credible.

The spatial distribution of LIS flashes during 2013–14 is shown in Fig. 5a, where each grid square is 1° × 1°. The 2754 LIS flashes matched by the WWLLN account for 2.42% of the total 113 970 LIS flashes. On the Tibetan Plateau (shown by the thick black line in Fig. 5), there are 457 matched flashes, 2.62% of the 17 475 LIS flashes in the same region. Figure 5b displays the spatial distribution of the ratio of matched LIS flashes to all LIS flashes. The ratio is generally lower than 10% in most regions of the plateau, except in some grid cells with relatively low total flash numbers.

According to the previous study (e.g., Qie et al. 2003), the diurnal lightning activity peaks in different regions of the Tibet Plateau all occurred during the afternoon of the local time. Therefore, we can assume that the DE of the LIS was constant through the plateau; then, Fig. 5b also shows the spatial distribution of the relative DE of

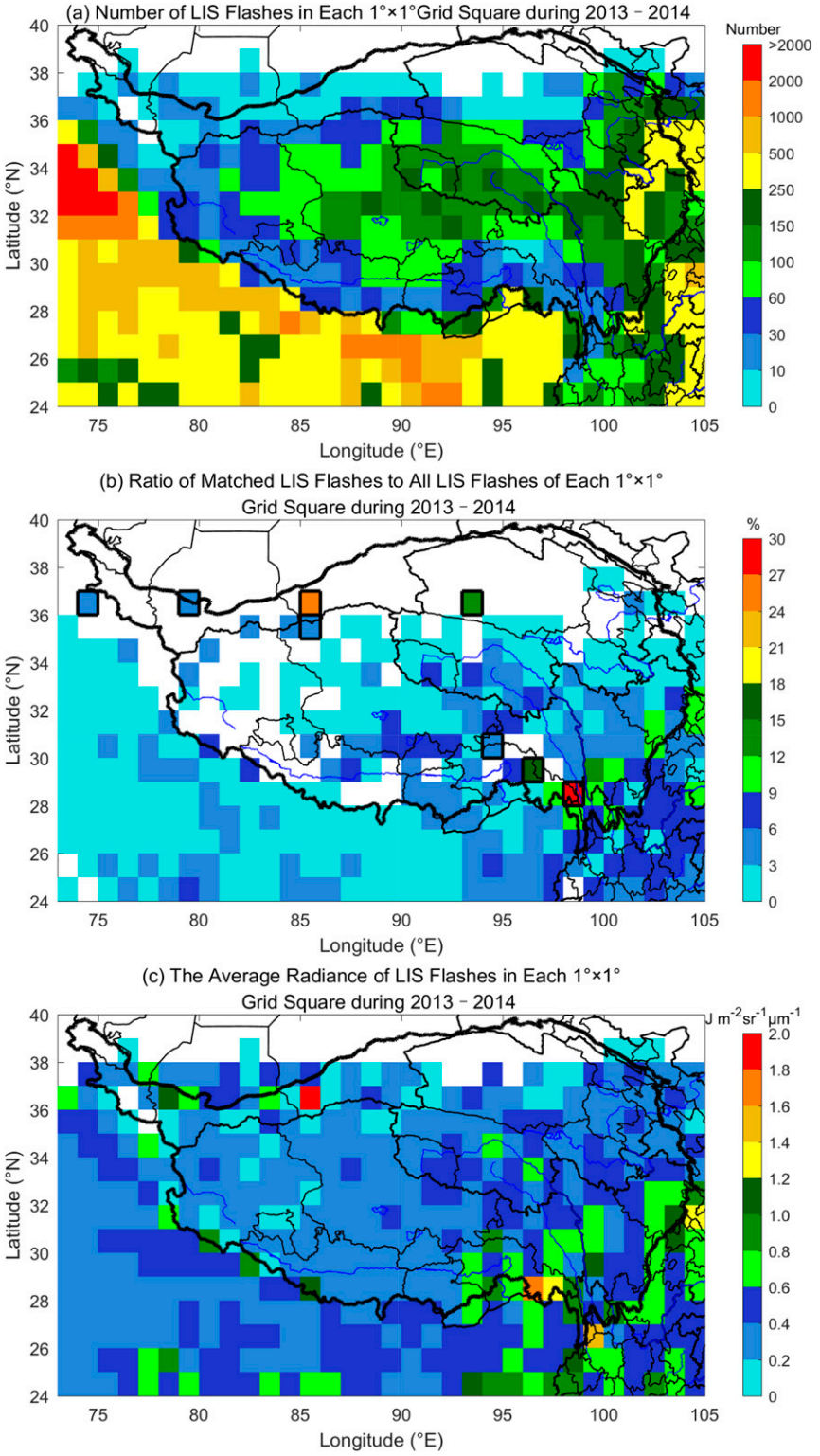

FIG. 5. (a) Spatial distribution of LIS flashes, (b) ratio of matched LIS flashes to all LIS flashes, and (c) average radiance of LIS flashes during 2013–14. In (b) the ratio is calculated by dividing the sum of the matched LIS flashes by the sum of all LIS flashes within $1° \times 1°$ grid cells. Grid cells outlined in black in (b) have fewer than 20 LIS flashes. Because of the small sample size in these grid cells, their flash ratios are highly variable.

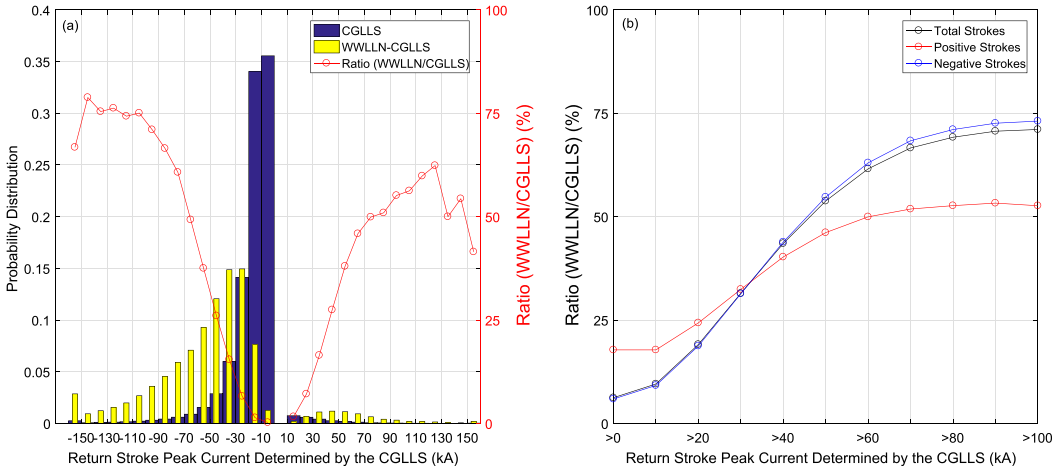

FIG. 6. (a) Distribution of all CGLLS return strokes and CGLLS return strokes matched by the WWLLN, and the ratio of the WWLLN matched return strokes to all CGLLS return strokes in different peak current intervals. (b) The ratio as a function of peak current amplitude. In (a), all the CGLLS return strokes (blue bars), the return strokes also detected by the WWLLN (yellow bars), and the ratio of WWLLN return strokes to all CGLLS return strokes (red dotted line) are denoted. In (b), the ratio for total (black), positive (red), and negative (blue) return strokes is shown.

WWLLN for total lightning. It decreases with the direction from the east to the west, while the largest DE are located southeast of the plateau. It is certain that the DE of WWLLN is impacted by the layout of the sensors. Meanwhile, the regional differences in the properties of lightning discharge may also play an important role in deciding the DE of WWLLN. Figure 5c exhibits the spatial distribution of the average radiance of the LIS flashes, which shows a very similar pattern to the relative DE of WWLLN in Fig. 5b. That is, the high DE of WWLLN occur in the area where the lightning discharge is generally strong and vice versa.

5. Results and discussion

The distance between neighboring WWLLN substations is generally on the order of 1000 km, which means that the lightning strokes detected by the WWLLN are more likely to have strong discharge intensity. Figure 6a shows the distribution of all CGLLS return strokes and CGLLS return strokes matched by the WWLLN in different peak current intervals, together with the ratio of matched return strokes to all return strokes. For all the CGLLS return stroke data, the average peak currents of positive and negative return strokes are 37.91 and −18.38 kA, respectively. The vast majority (>70%) of the samples have an absolute value less than 20 kA. However, the average peak currents of WWLLN matched strokes are 62.43 (positive) and −56.74 kA (negative), with the peak distribution intervals corresponding to 40 to 50 and −30 to −20 kA, respectively.

The average return stroke peak current detected by the WWLLN is significantly higher than that detected by the CGLLS, which suggests that the WWLLN is indeed more likely to detect high-current discharges. This result is consistent with previous studies (Lay et al. 2004; Rodger et al. 2004, 2006; Jacobson et al. 2006; Abreu et al. 2010).

Moreover, the ratio of matched return strokes to the total return strokes (Fig. 6a) shows that WWLLN's DE increases significantly with increasing return stroke peak current (the fluctuations in the curve for values greater than 100 kA are attributed to the small sample size), and the growth rate on the negative side tends to be higher than that on the positive side, especially when the peak current amplitude exceeds 60 kA. In other words, the WWLLN's DE for positive strokes with a high peak current is lower than that for negative strokes. A similar distribution has also been reported by Abarca et al. (2010, their Fig. 3b). Figure 6b embodies this characteristic more intuitively. With increasing peak current amplitude, the ratio of negative CGLLS return strokes also detected by the WWLLN to all negative CGLLS return strokes grows faster than that of positive return strokes. Overall, the WWLLN detects only 0.80% (not shown) of the return strokes from all CGLLS return stroke data when the peak current is less than 20 kA, while when the peak current is greater than 50, 75, and 100 kA, the corresponding values are 53.8%, 68.0%, and 71.1%, respectively.

The analysis of the results matched with the LIS also indicates that the WWLLN mainly detects strong flash events. Table 2 compares the lightning parameters of the LIS flashes also detected by the WWLLN with those detected only by the LIS in all LIS flashes. The flashes

TABLE 2. Average parameter characteristics of LIS flashes detected (matched) and not detected (not matched) by the WWLLN. The "25th" and "75th" are the 25th and 75th percentiles, respectively.

	Matched (2754)			Not matched (111 216)			
	Mean	25th	75th	Mean	25th	75th	Average multiple
Groups (N)	12.49	3	15	8.31	2	10	1.50
Events (N)	85.99	15	96	31.14	7	32	2.76
Duration (ms)	269.2	62.8	399.0	211.1	48.2	306.0	1.27
Area (km^2)	554.08	196.39	693.54	208.86	93.59	254.71	2.65
Radiance ($J\,m^{-2}\,sr^{-1}\,\mu m^{-1}$)	1.687	0.115	1.338	0.385	0.051	0.321	4.38

also detected by the WWLLN include significantly more groups and "events," and their duration, area, and radiance are respectively 1.27, 2.65, and 4.38 times greater than those not detected by the WWLLN.

For any lightning detection system, the ability to detect low intensity lightning discharge events is relatively weak. Therefore, we assume that lightning events that the CGLLS or the LIS did not detect cannot theoretically be detected by the WWLLN. Based on this premise, we consider the DE of the CGLLS and the LIS, as well as the WWLLN matched ratio, to give further estimates of the DE of the WWLLN for CG lightning and total lightning.

According to Chen et al. (2012), the DE of their lightning location system used in Guangdong, which employed the same technique as CGLLS in this analysis, was 94% for CG lightning. While the WWLLN detected 9.97% of all CGLLS CG flash records in the MSTP region, the absolute DE of the WWLLN for CG lightning was thus estimated to be 9.37%. Besides, a total number of 497 LIS flashes were also observed by the WWLLN in the Tibetan Plateau region (Fig. 1). Referring to the LIS daytime DE of 73% and nighttime DE of 93%, as suggested by Boccippio et al. (2002), and the local time of the LIS flash records, the number of actually happened flash could also be estimated. The absolute DE of the WWLLN for total lightning in the Tibetan Plateau was estimated to be 2.03%. For the MSTP region, the absolute DE was estimated to be 2.58%.

Table 3 lists the results of this study and previous analyses of WWLLN detection performance in different regions. With increasing numbers of WWLLN sensors, the DE and LA have improved steadily overall. In this study the DE for total lightning relative to the LIS in the Tibetan Plateau region is 2.62%. Correspondingly, Rudlosky and Shea (2013) found a WWLLN DE of 5.2% for total lightning relative to the LIS over Western Hemisphere land, and Thompson et al. (2014) found for South and North America that the relative DEs of the WWLLN for total lightning compared with the LIS were 13.2% and 6.2%, respectively. These results indicate that the WWLLN has a lower DE for total lightning in the Tibet Plateau than in the Western Hemisphere. This conclusion is also consistent with the global distribution of relative WWLLN DE reported by Hutchins et al. (2012), in which the relative DE value was lower over the Tibetan Plateau (Fig. 7 in Hutchins et al. 2012).

However, the relative CG DE of 9.97% and the absolute CG DE of 9.37% in the MSTP region are comparable to the relative DE of 10.30% calculated by Abarca et al. (2010) in the United States during 2008–09. Taking into account the increase in the number of sensors, the WWLLN DE for CG lightning may also be lower over the plateau. As for the LA, for studies after 2009 the LA of the WWLLN relative to other networks is concentrated around 10 km, consistent with the results of the present study.

The low DE of WWLLN over the plateau should be partly attributed to the small number of WWLLN sensors around this region [Fig. 1 in Soula et al. (2016) and the website of the WWLLN]. Another possibility may be associated with the weak lightning discharge intensity over the plateau. Beirle et al. (2014), in their Fig. 2d, gave the global distribution of the radiance per flash detected by the LIS. It apparently explored that the flashes over the plateau were of weak radiance relative to those over the places listed in Table 3.

By matching WWLLN and CGLLS data in the MSTP region, WWLLN stroke data were divided into CG return stokes and IC pulses. We then grouped WWLLN strokes into flashes, employing the method described in section 2a, and determined whether these flashes were CG or IC. In the MSTP region, 81 105 strokes were grouped into 62 185 flashes, with 44 762 CG flashes and 17 423 IC flashes. The proportion of CG flash data to all WWLLN flash data is 71.98% in the MSTP region.

Based on the components (IC and CG flashes) of the WWLLN data and the estimated total flash DE and CG flash DE of the WWLLN, the ratio of IC flashes to CG flashes (i.e., Z value) in the MSTP region can be estimated according to the following method:

Assuming that the number of total flashes in the MSTP region is N, the number of total flashes (N_{WL}) and

TABLE 3. Summary of comparisons of the WWLLN with other networks.

Study	Country, regional network	Region of interest	Matched data	Criteria for coincidence[a] [*T*], [*S*]	Period	No. of WWLLN sensors[b]	DE[c] (%)**[*A*]** *[R]*	LA[d] (km)
Lay et al. (2004)	Brazil, BIN	15–25°S, 40–55°W	CG lightning stroke	3 ms, 50 km	6–7, 14, 20–21 Mar 2003	11	Total = **0.3** CG = *0.5*	20.25 ± 13.5, lat = 7.3, lon = 3.2
Rodger et al. (2004)	Australia, Kattron	Southeast Australia	Total lightning stroke	3 ms, 50 km	23–24 Jan 2002	11	Total = *1.4*	30
Rodger et al. (2006)	New Zealand, NZLDN	34°–49°S, 165–180°E	Total lightning stroke	0.5 ms	13 Jan 2004	20	Total = *2.7*; Total = **5.4** CG = *2.9* IC = *1.0*	—[e]
Jacobson et al. (2006)	United States, LASA	≤400-km radius circle, centered at 29°N, 82°W	Total lightning stroke	1 ms, 100 km	27 Apr–30 Sep 2004	19	Total = *0.8* CG = *1.3* IC = *0.5*	15–20
Abreu et al. (2010)	Canada, CLDN	41.7°–45.7°N, 77.4°–81.4°W	Total lightning stroke	0.5 ms	1 May–31 Aug 2008	29	Total = *2.8*	7.24 ± 6.34, lat = 1.62 ± 6.71, lon = −3.14 ± 5.91
Abarca et al. (2010)	United States, NLDN	25°–45°N, 75°–125°W	CG lightning stroke	0.5 s, 20 km	5 Apr 2006–31 Mar 2009	38	[f]Total = *6.2* [f]CG = *10.3* [f]IC = *4.8*	Lat = 4.98 lon = 4.03
Rudlosky and Shea (2013)	LIS	Western Hemisphere 38°N–38°S	LIS flash	330 ms, 25 km	1 Jan 2009–1 Jan 2012	NA	Total = *7.5* [g]Land = *5.2* [g]Ocean = *14.7*	11
Thompson et al. (2014)	LIS	Western Hemisphere 38°N–38°S	LIS group	0.4 s[h] [*S*] = 0.15°	1 Jan 2010–30 Jun 2011	>38	Total = *11.1* [i]NAL = *13.2* [i]SAL = *6.2*	—
This study	China, CGLLS;	MSTP region	CG lightning stroke	0.5 ms, 50 km	1 Jan 2013–1 Jan 2015;	>70	CG = *9.97* CG = **9.37**;	9.97 ± 9.54, lat = 1.09 ± 9.96, lon = 0.72 ± 9.44
	LIS	24–40°N, 93–105°E	LIS flash	330 ms, 25 km	1 Jan 2013–1 Jan 2014		Total= *2.42* Total = **2.13**	10.93 ± 5.92, lat = 0.62 ± 8.56, lon = −1.62 ± 8.69

[a] The time and space criteria for matching are denoted by [*T*] and [*S*], respectively.
[b] Number of WWLLN sensors at the time of study.
[c] Total, CG, and IC indicate the DE for total, CG, and IC lightning, respectively. The boldface and italic values in this column indicate the absolute DE ([**A**]) and relative DE ([*R*]), respectively.
[d] Lat and Lon mean latitudinal and longitudinal spatial location separation magnitude, respectively.
[e] NA indicates that no data are available in the study.
[f] Calculated based only on the data during 2008–09.
[g] Land or ocean indicates DE for total lightning over land or ocean.
[h] 0.15° is within a distance of 0.15° longitude and latitude.
[i] NAL or SAL indicates DE for total lightning over North American land or South American land, respectively.

CG flashes (N_{WLCG}) detected by the WWLLN can be calculated by the following equations:

$$N_{WL} = \alpha_T N,$$
$$N_{WLCG} = \alpha_T \beta_{CG} N,$$

where α_T is the total flash DE of the WWLLN and β_{CG} is the proportion of CG flash data in the WWLLN flash data.

Taking the CG flash DE α_{CG} into consideration, the number of the actual CG flash (N_{CG}) should be

$$N_{CG} = \frac{N_{WLCG}}{\alpha_{CG}} = \frac{\alpha_T \beta_{CG} N}{\alpha_{CG}}.$$

Therefore, the ratio of IC flashes to CG flashes (Z value) can be calculated by

$$Z = \frac{N - N_{CG}}{N_{CG}} = \frac{\alpha_{CG}}{\alpha_T \beta_{CG}} - 1.$$

Finally, the Z value in the MSTP region was estimated to be about 4.05. This value is in good agreement with the distribution Z-value curve with latitude plotted by Boccippio et al. (2001, their Fig. 1). In contrast, Mackerras et al. (1998) estimated the global average Z value to be 3.53, Rivas Soriano and de Pablo (2007) calculated a Z value of 3.48 in the Iberian Peninsula, and de Souza et al. (2009) found that the spatial distribution of Z varies widely in Brazil, ranging from 2 to 12.

6. Summary

This study has compared 3 years (2013–15) of data from the WWLLN and the CGLLS, and 2 years (2013–14) of data from the WWLLN and the LIS over the Tibetan Plateau and the surrounding area. For the first time, the performance of the WWLLN in the Tibetan Plateau area is analyzed and the following results are obtained.

In the MSTP region, the WWLLN observed 9.97% of the CGLLS flashes, and the average spatial location separation magnitude compared with the CGLLS was 9.97 km. Over the Tibetan Plateau, the WWLLN detected 2.62% of the LIS flashes, and its average spatial location separation magnitude was 10.93 km. The DE of WWLLN decreases with direction from east to west over the plateau, which is consistent with the spatial change of the average flash radiance.

The DE of the WWLLN increases with increasing return stroke peak current. According to the results of the CGLLS, in the MSTP region the average peak current of the WWLLN strokes is 62.43 kA for positive strokes and −56.74 kA for negative strokes, and the corresponding peak distribution intervals are 40 to 50 and −30 to −20 kA. The WWLLN detects only 0.80% of CGLLS return strokes when the peak current is less than 20 kA, but it detects 53.8%, 68.0%, and 71.1% for peak current greater than 50, 75, and 100 kA, respectively. LIS flashes also detected by the WWLLN have significantly greater scale and stronger optical radiation energy, and their duration, area, and radiance are respectively 1.27, 2.65, and 4.38 times greater than those not detected by the WWLLN.

Considering the estimates of CGLLS and LIS DE in previous studies (Boccippio et al. 2002; Chen et al. 2012), and combining the matching ratio of the WWLLN and the CGLLS or the LIS, we estimate a WWLLN DE of 9.37% for CG lightning and 2.58% for total lightning in the MSTP region. In the selected region of the Tibetan Plateau, WWLLN DE for total lightning is 2.03%. The low DE of WWLLN may be partly attributed to the weaker lightning discharge intensity over the plateau relative to other places.

The CG flashes account for 71.98% of all WWLLN flash data in the MSTP region. Combined with the DE estimates, it is estimated that the ratio of IC flashes to CG flashes is about 4.05 in the MSTP region.

Acknowledgments. This work was supported by the National Natural Science Foundation of China (91537209 and 41675005), the National Key Research and Development Program of China (2017YFC1501503), and the Basic Research Fund of the Chinese Academy of Meteorological Sciences (2016Z002 and 2015Z006).

We thank the institutions and organizations that provided the data used in this study. The CGLLS CG data were provided by Wuhan NARI Company Ltd. of the State Grid Electric Power Research Institute. The WWLLN lightning data were provided by the World Wide Lightning Location Network (http://wwlln.net/), a collaboration among over 50 universities and institutions. The data for TRMM/LIS lightning were required as part of TRMM. TRMM is an international project jointly sponsored by the Japan National Space Development Agency (NASDA) and the National Aeronautics and Space Administration's (NASA) Office of Earth Science. The data can be accessed from https://doi.org/10.5281/zenodo.1213027 or from the corresponding author (zhengdong@cma.gov.cn).

REFERENCES

Abarca, S. F., K. L. Corbosiero, and T. J. Galarneau, 2010: An evaluation of the Worldwide Lightning Location Network (WWLLN) using the National Lightning Detection Network (NLDN) as ground truth. *J. Geophys. Res.*, **115**, D18206, https://doi.org/10.1029/2009JD013411.

Abreu, D., D. Chandan, R. H. Holzworth, and K. Strong, 2010: A performance assessment of the World Wide Lightning

Location Network (WWLLN) via comparison with the Canadian Lightning Detection Network (CLDN). *Atmos. Meas. Tech.*, **3**, 1143–1153, https://doi.org/10.5194/amt-3-1143-2010.

Beirle, S., W. Koshak, R. Blakeslee, and T. Wagner, 2014: Global patterns of lightning properties derived by OTD and LIS. *Nat. Hazards Earth Syst. Sci.*, **14**, 2715–2726, https://doi.org/10.5194/nhess-14-2715-2014.

Boccippio, D. J., K. L. Cummins, H. J. Christian, and S. J. Goodman, 2001: Combined satellite- and surface-based estimation of the intracloud–cloud-to-ground lightning ratio over the continental United States. *Mon. Wea. Rev.*, **129**, 108–122, https://doi.org/10.1175/1520-0493(2001)129<0108:CSASBE>2.0.CO;2.

——, W. J. Koshak, and R. J. Blakeslee, 2002: Performance assessment of the Optical Transient Detector and Lightning Imaging Sensor. Part I: Predicted diurnal variability. *J. Atmos. Oceanic Technol.*, **19**, 1318–1332, https://doi.org/10.1175/1520-0426(2002)019<1318:PAOTOT>2.0.CO;2.

Bürgesser, R. E., 2017: Assessment of the World Wide Lightning Location Network (WWLLN) detection efficiency by comparison to the Lightning Imaging Sensor (LIS). *Quart. J. Roy. Meteor. Soc.*, **143**, 2809–2817, https://doi.org/10.1002/qj.3129.

Cao, D., 2016: The development of product algorithm of the Fengyun-4 geostationary lightning imager (in Chinese). *Adv. Meteor. Sci. Tech.*, **6**, 94–98.

Cecil, D. J., D. E. Buechler, and R. J. Blakeslee, 2014: Gridded lightning climatology from TRMM-LIS and OTD: Dataset description. *Atmos. Res.*, **135–136**, 404–414, https://doi.org/10.1016/j.atmosres.2012.06.028.

Chen, L., Y. Zhang, W. Lu, D. Zheng, Y. Zhang, S. Chen, and Z. Huang, 2012: Performance evaluation for a lightning location system based on observations of artificially triggered lightning and natural lightning flashes. *J. Atmos. Oceanic Technol.*, **29**, 1835–1844, https://doi.org/10.1175/JTECH-D-12-00028.1.

Chen, S. M., Y. Du, L. M. Fan, H. M. He, and D. Z. Zhong, 2002: Evaluation of the Guang Dong lightning location system with transmission line fault data. *IEE Proc.: Sci. Meas. Technol.*, **149**, 9–16, https://doi.org/10.1049/ip-smt:20020131.

Christian, H. J., and Coauthors, 1999: The Lightning Imaging Sensor. *11th International Conference on Atmospheric Electricity*, H. J. Christian, Ed., NASA Conf. Publ. NASA/CP—1999-209261, 746–749.

——, and Coauthors, 2003: Global frequency and distribution of lightning as observed from space by the Optical Transient Detector. *J. Geophys. Res.*, **108**, 4005, https://doi.org/10.1029/2002JD002347.

Cummins, K. L., M. J. Murphy, E. A. Bardo, W. L. Hiscox, R. B. Pyle, and A. E. Pifer, 1998: A combined TOA/MDF technology upgrade of the U.S. National Lightning Detection Network. *J. Geophys. Res.*, **103**, 9035–9044, https://doi.org/10.1029/98JD00153.

de Souza, P. E., Jr., O. Pinto, I. R. C. A. Pinto, N. J. Ferreira, and A. F. dos Santos, 2009: The intracloud/cloud-to-ground lightning ratio in Southeastern Brazil. *Atmos. Res.*, **91**, 491–499, https://doi.org/10.1016/j.atmosres.2008.06.011.

Dowden, R. L., J. B. Brundell, and C. J. Rodger, 2002: VLF lightning location by time of group arrival (TOGA) at multiple sites. *J. Atmos. Sol.-Terr. Phys.*, **64**, 817–830, https://doi.org/10.1016/S1364-6826(02)00085-8.

——, and Coauthors, 2008: World-wide lightning location using VLF propagation in the Earth-ionosphere waveguide. *IEEE Antennas Propag. Mag.*, **50**, 40–60, https://doi.org/10.1109/MAP.2008.4674710.

Flohn, H., and E. R. Reiter, 1968: Contributions to a meteorology of the Tibetan Highlands. Colorado State University Atmospheric Science Paper 130, 120 pp.

Hutchins, M. L., R. H. Holzworth, J. B. Brundell, and C. J. Rodger, 2012: Relative detection efficiency of the World Wide Lightning Location Network. *Radio Sci.*, **47**, RS6005, https://doi.org/10.1029/2012RS005049.

——, ——, K. S. Virts, J. M. Wallace, and S. Heckman, 2013: Radiated VLF energy differences of land and oceanic lightning. *Geophys. Res. Lett.*, **40**, 2390–2394, https://doi.org/10.1002/grl.50406.

Jacobson, A. R., R. Holzworth, J. Harlin, R. Dowden, and E. Lay, 2006: Performance assessment of the World Wide Lightning Location Network (WWLLN), using the Los Alamos Sferic Array (LASA) as ground truth. *J. Atmos. Oceanic Technol.*, **23**, 1082–1092, https://doi.org/10.1175/JTECH1902.1.

Lay, E. H., R. H. Holzworth, C. J. Rodger, J. N. Thomas, O. Pinto Jr., and R. L. Dowden, 2004: WWLL global lightning detection system: Regional validation study in Brazil. *Geophys. Res. Lett.*, **31**, L03102, https://doi.org/10.1029/2003GL018882.

Mach, D. M., H. J. Christian, R. J. Blakeslee, D. J. Boccippio, S. J. Goodman, and W. L. Boeck, 2007: Performance assessment of the Optical Transient Detector and Lightning Imaging Sensor. *J. Geophys. Res.*, **112**, D09210, https://doi.org/10.1029/2006JD007787.

Mackerras, D., M. Darveniza, R. E. Orville, E. R. Williams, and S. J. Goodman, 1998: Global lightning: Total, cloud and ground flash estimates. *J. Geophys. Res.*, **103**, 19 791–19 809, https://doi.org/10.1029/98JD01461.

Qi, P., D. Zheng, Y. Zhang, and L. Gao, 2016: Climatological characteristics and spatio-temporal correspondence of lightning and precipitation over the Tibetan Plateau (in Chinese). *J. Appl. Meteor. Sci*, **27**, 488–497.

Qie, X., and R. Toumi, 2003: Lightning activities on Qinghai-Xizang Plateau as observed by satellite-based lightning imaging sensor (in Chinese). *Plateau Meteor.*, **22**, 288–294.

——, ——, and T. Yuan, 2003: Lightning activities on the Tibetan Plateau as observed by the lightning imaging sensor. *J. Geophys. Res.*, **108**, 4551, https://doi.org/10.1029/2002JD003304.

Rivas Soriano, L., and F. de Pablo, 2007: Total flash density and the intracloud/cloud-to-ground lightning ratio over the Iberian Peninsula. *J. Geophys. Res.*, **112**, D13114, https://doi.org/10.1029/2006JD007624.

Rodger, C. J., J. B. Brundell, R. L. Dowden, and N. Thomson, 2004: Location accuracy of long distance VLF lightning location network. *Ann. Geophys.*, **22**, 747–758, https://doi.org/10.5194/angeo-22-747-2004.

——, ——, and ——, 2005: Location accuracy of VLF World-Wide Lightning Location (WWLL) network: Post-algorithm upgrade. *Ann. Geophys.*, **23**, 277–290, https://doi.org/10.5194/angeo-23-277-2005.

——, S. Werner, J. B. Brundell, E. H. Lay, N. R. Thomson, R. H. Holzworth, and R. L. Dowden, 2006: Detection efficiency of the VLF World-Wide Lightning Location Network (WWLLN): Initial case study. *Ann. Geophys.*, **24**, 3197–3214, https://doi.org/10.5194/angeo-24-3197-2006.

——, J. B. Brundell, R. H. Holzworth, and E. H. Lay, 2009: Growing detection efficiency of the World Wide Lightning Location Network. *AIP Conf. Proc.*, **1118**, 15–20, https://doi.org/10.1063/1.3137706.

Rudlosky, S. D., and D. T. Shea, 2013: Evaluating WWLLN performance relative to TRMM/LIS. *Geophys. Res. Lett.*, **40**, 2344–2348, https://doi.org/10.1002/grl.50428.

Soula, S., J. K. Kasereka, J. F. Georgis, and C. Barthe, 2016: Lightning climatology in the Congo Basin. *Atmos. Res.*, **178–179**, 304–319, https://doi.org/10.1016/j.atmosres.2016.04.006.

Thompson, K. B., M. G. Bateman, and L. D. Carey, 2014: A comparison of two ground-based lightning detection networks against the satellite-based Lightning Imaging Sensor (LIS). *J. Atmos. Oceanic Technol.*, **31**, 2191–2205, https://doi.org/10.1175/JTECH-D-13-00186.1.

Ushio, T., S. Heckman, K. Driscoll, D. Boccippio, H. Christian, and Z. Kawasaki, 2002: Cross-sensor comparison of the Lightning Imaging Sensor (LIS). *Int. J. Remote Sens.*, **23**, 2703–2712, https://doi.org/10.1080/01431160110107789.

Xia, R., D. Zhang, and B. Wang, 2015: A 6-yr cloud-to-ground lightning climatology and its relationship to rainfall over central and eastern China. *J. Appl. Meteor. Climatol.*, **54**, 2443–2460, https://doi.org/10.1175/JAMC-D-15-0029.1.

Yanai, M., and C. Li, 1994: Mechanism of heating and the boundary layer over the Tibetan Plateau. *Mon. Wea. Rev.*, **122**, 305, https://doi.org/10.1175/1520-0493(1994)122<0305:MOHATB>2.0.CO;2.

Yang, X., J. Sun, and W. Li, 2015: An analysis of cloud-to-ground lightning in China during 2010–13. *Wea. Forecasting*, **30**, 1537–1550, https://doi.org/10.1175/WAF-D-14-00132.1.

Zhang, Y.-L., B.-Y. Li, and D. Zheng, 2002: A discussion on the boundary and area of the Tibetan Plateau in China (in Chinese). *Geogr. Res.*, **21** (1), 1–8.

Zheng, D., Y. Zhang, Q. Meng, L. Chen, and J. Dan, 2016: Climatological comparison of small- and large-current cloud-to-ground lightning flashes over southern China. *J. Climate*, **29**, 2831–2848, https://doi.org/10.1175/JCLI-D-15-0386.1.